JOURNAL OF SOLID STATE CHEMISTRY **139,** 304–309 (1998)
ARTICLE NO. SC987845

Single-Crystal Growth and Structure Determination of a New Oxide Apatite, $NaLa_9(GeO_4)_6O_2$

Masaru Takahashi,*,[1] Kazuyoshi Uematsu,† Zuo-Guang Ye,† and Mineo Sato†

*Department of Active Material Chemistry, Graduate School of Science and Technology, Niigata University, 8050 Ikarashi 2-nocho, Niigata-shi 950-21, Japan; and †Department of Chemistry and Chemical Engineering, Faculty of Engineering, Niigata University, 8050 Ikarashi 2-nocho, Niigata-shi 950-21, Japan

Received June 6, 1997; in revised form April 1, 1998; accepted April 13, 1998

$NaLa_9Ge_6O_{26}$, hexagonal, $a = 0.9883(2)$ nm, $c = 0.7267(3)$ nm, $V = 6.147(3) \times 10^5$ nm^3, space group $P6_3/m$, $Z = 1$, $D_{calc} = 5.739$ g cm^{-3}, $\lambda(MoK\alpha) = 0.071069$ nm, $\mu = 225.16$ cm^{-1}, $F(000) = 924$, $T = 298$ K, $R = 0.031$, $R_w = 0.037$ for 966 measured unique reflections. Single crystals of $NaLa_9Ge_6O_{26}$ were grown both by a high-temperature flux method and from a melt system. The crystal structure was found to be similar to that of the silicate oxyapatite $NaY_9Si_6O_{26}$. The 4*f* cation sites are occupied disorderedly by La and Na. On the other hand, the 6*h* cation sites are occupied by La only. This compound constitutes a new member of the oxyapatite-type structure family with general formula $A_x\,Ln_{10-x}B_6O_{24}O_{3-x}$ ($x = 1$, A = alkali metals, B = Si, Ge, Ln = rare earth). © 1998 Academic Press

***Key Words*: single-crystal growth; crystal structure; oxyapatite; $NaLa_9(GeO_4)_6O_2$.**

1. INTRODUCTION

Data on the synthesis and characterization of some ternary phases of the ternary system Na_2O–Y_2O_3–SiO_2 have been reported by Cervantes *et al.* (1), with seven existing compounds: $NaYSiO_4$, $NaYSi_2O_6$, $Na_3YSi_2O_7$, $Na_3YSi_3O_9$, $Na_5YSi_4O_{12}$, $Na_9YSi_6O_{18}$, and $NaY_9Si_6O_{26}$. The oxyapatite phase, $NaY_9Si_6O_{26}$, seems to be most interesting to us because of potential luminescent properties. The structure of this compound was refined by Gunawardane *et al.* (2) with a hexagonal lattice [$a = 0.9334(2)$ nm, $c = 0.6759(1)$ nm, space group $P6_3/m$]. This structure was reported to have two sets of crystallographically independent positions for Y atoms in the unit cell. One is coordinated by seven O atoms at a mean distance of 0.242 nm, with only one relatively short distance of 0.220 nm. The other is surrounded by nine O atoms at a mean distance of 0.240 nm, with six of these O atoms at a shorter distance (0.237 nm) and the remaining three O atoms at a longer distance (~0.278 nm). Therefore, the nine coordinated Y atom sites are very distorted.

Many apatite-type compounds are known to have good luminescent properties. The luminescent properties of $M^+Ln_9(SiO_4)_6O_2$ (M^+ = Li, Na) and $M_2^{2+}Ln_8(SiO_4)_6O_2$ (M^{2+} = Mg, Ca) activated by Eu^{3+} have been discussed by Blasse (3). As stated above, the apatite structure contains two different sites for the larger cations. Blasse showed that the principle of local charge compensation could predict site occupation. This is especially important in the interpretation of the luminescent properties of a number of apatites. The predictions were compared with experimental data. For example, the $^5D_0$–$^7F_0$ emission of Eu^{3+} in the $LiLa_9(SiO_4)_6O_2$ compound is rather intense, indicating a strong linear crystal-field component at the Eu^{3+} ion. It is quite obvious that this is the case for the 6*h* site whose symmetry is C_s with one free oxygen ion in the symmetry plane. The agreement was therefore satisfactory. Moreover, recently Fleet and Pan reported that Na atoms are preferred on the 4*f* site in the fluorapatite structure (4). On the other hand, the photoluminescence of $Na_3YSi_3O_9$ activated by Eu^{3+} and Bi^{3+} was recently reported by Kim *et al.* (5). The optical characteristics of Bi^{3+} and Eu^{3+} and the energy transfer between the incorporated ions in this compound were examined.

We have been particularly interested in the germanates containing rare earth analogues in the Na_2O–Ln_2O_3–SiO_2 system, with a view toward studying the structural and luminescent properties by suitable activation. From the viewpoint of chemical synthesis, especially the growth of single crystals, it is essential to choose an appropriate flux composition. In the PbO–B_2O_3 flux system, there are four compounds of which PbB_4O_7 has the highest melting point of 1041 K. On the B_2O_3-rich side, a large liquid immiscibility region exists up to 1073 K. The PbO–B_2O_3 system was used for seeded growth and for low working temperature. A compromise must, however, be found between the high viscosity at low temperatures (below 1273 K) and the high volatility at high temperatures (above 1473 K) (6). Schieber

[1] To whom correspondence should be addressed.

0022-4596/98 $25.00

(7) proposed $PbO–B_2O_3$ as a fluorine-free solvent for the growth of rare-earth magnetic garnets, $Ln_3Fe_5O_{12}$. From the above mentioned characteristics, this flux was considered to be effective for the crystal growth of oxyapatite-containing rare earth.

The present paper reports on the single-crystal growth and structure determination of a new oxyapatite, $NaLa_9Ge_6O_{26}$, in the $Na_2O–La_2O_3–GeO_2$ system. Structural features are discussed in comparison with the silicate analogue $NaY_9Si_6O_{26}$ (2).

2. EXPERIMENTAL AND RESULTS

2.1. Solid-State Synthesis

The Polycrystalline $NaLa_9Ge_6O_{26}$ was first synthesized by conventional solid-state reactions. The starting materials were reagent-grade Na_2CO_3, La_2O_3, and GeO_2. Excess amounts of Na_2CO_3 (30 mol%) were added to compensate for the loss due to evaporation of Na_2O. The powders were intimately ground, pressed into the form of pellets, preheated in air at 1173 K in alumina crucibles for 6*h*, and then sintered at 1373 K for 1 h. The *d* values of the lines were obtained from the powder diffraction data of $NaLa_9Ge_6O_{26}$, measured using an X-ray diffractometer (Rigaku, RAD-rA) with Cu$K\alpha_1$ radiation at 40 kV and 40 mA (see Table 1). X-ray powder diffraction patterns indicated the formation of a single apatite phase.

TABLE 1
Comparison of Observed Values of d_{obs} and I_{obs} of $NaLa_9(GeO_4)_6O_2$ with Calculated I_{calc} (at Room Temperature, Cu$K\alpha_1$)

hkl	*d* (Å)	I_{obs}	I_{calc}
101	5.5416	1	1
200	4.2853	15	15
111	4.0896	5	5
002	3.6322	33	32
102	3.3442	31	30
120	3.2394	30	29
210	3.2394	9	9
211	2.9586	50	49
121	2.9586	100	99
112	2.9280	68	68
300	2.8569	43	42
202	2.7708	8	8
130	2.3771	5	5
310	2.3771	3	3
221	2.3420	10	9
311	2.2592	3	3
302	2.2455	1	1
113	2.1750	4	4
400	2.1427	5	4
203	2.1082	2	1
401	2.0551	1	1
222	2.0448	35	32
132	1.9890	2	2
312	1.9890	8	8
320	1.9662	2	2
213	1.9395	16	16
123	1.9395	34	33
231	1.8979	12	11
321	1.8979	9	8
410	1.8703	16	16
140	1.8703	6	6
402	1.8455	24	23
004	1.8161	18	18
141	1.8112	1	1

2.2. Single-Crystal Growth and Optical Properties of $NaLa_9Ge_6O_{26}$

Single crystals of $NaLa_9Ge_6O_{26}$ were synthesized both from a high-temperature solution growth and from a melt growth. In the flux method, the mixture ($PbO–B_2O_3–Na_2O$) was chosen as flux. This flux retains the advantages of the $PbO–B_2O_3$ mixture, in particular, with respect to low melting points and high capacity to dissolve heavy compounds. The presence of Na_2O in the flux may create a milieu rich in alkaline metal and compensate for the evaporation of Na_2O. In the flux growth, mixtures of compound/flux (with a ratio of 3.08 : 1 in moles) were heated to 1223 K in Pt crucibles and then slowly cooled to 873 K at the rate of 5 K h^{-1}. In the melt growth, crystals were grown from a mixture of Na_2CO_3, La_2O_3, and GeO_2 with a large excess of Na_2CO_3 (200 mol%), which was heated to 1623 K in Pt crucibles and then slowly cooled to 1543 K at the rate of 1 K h^{-1}.

The grown crystals were found on the solidified liquid surface or crucible walls. They were removed in boiling water or in dilute HCl, then completely cleaned with dilute HCl to remove the residual flux. Transparent thin crystal plates were obtained by both growth techniques. The typical size of the crystals was $0.2 \times 0.1 \times 0.1\,mm^3$ (Fig. 1). The growth results were found to depend closely on the flux ratio. In the case of $PbO–B_2O_3–Na_2O$ flux only small crystals were obtained. Increasing the proportion of PbO led to larger crystals. $3PbO–B_2O_3–Na_2O$ flux was finally identified to be the best flux for the growth of germanate apatite.

Qualitative and quantitative chemical analyses were undertaken by electron probe microanalysis (EPMA) using a Shimadzu EPMA-8705. In the quantitative analysis, single crystals of Na, Ge, O (component), and metallic La were used as standards. The homogeneous composition of the grown crystals was determined with a Na : La : Ge : O ratio of close to 1 : 9 : 6 : 26, indicating the formula of an apatite phase, $NaLa_9Ge_6O_{26}$.

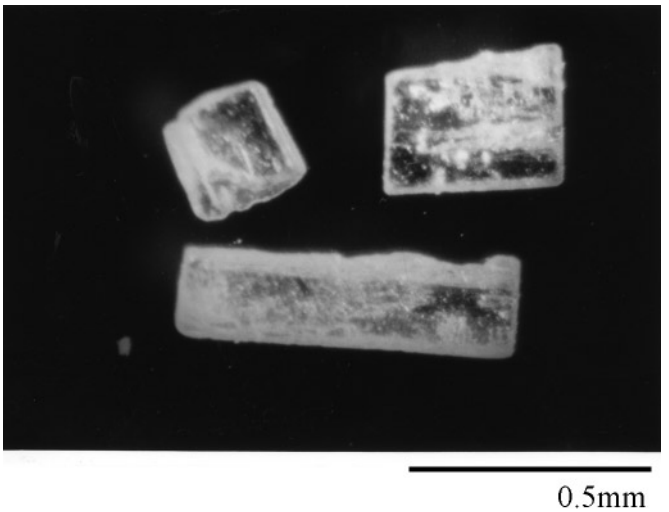

FIG. 1. Habits of some as-grown single crystals of the oxyapatite $NaLa_9(GeO_4)O_2$ from high-temperature solution.

Platelets about 30 μm thick were cut parallel to the principal {100} facets of the as-grown crystals, finely polished, and examined with a polarized light microscope (Olympus BX-60) in transmission. At room temperature single crystals of $NaLa_9Ge_6O_{26}$ show optically uniaxial negative character ($n_E < n_O$) with the optical axis (c axis) parallel to the dominant growth direction, as indicated in Fig. 2. The optical negative character reflects the anisotropic atomic arrangement of the apatite structure (see Section 2.3), with a larger polarizability for the atomic groups in the plane perpendicular to the c axis, hence a higher ordinary refractive index, n_O (8). The principal birefringence value was found to be $\Delta n = n_O - n_E = 3.0 \times 10^{-2}$. A slightly anisotropic absorption between $a(b)$ and c axes (dichroism) was observed with a single polarizer.

2.3. Single-Cyrstal Structure Determination

A colorless plate-like crystal of $NaLa_9Ge_6O_{26}$ having the approximate dimensions $0.15 \times 0.10 \times 0.10\,mm^3$ was mounted on a fine glass capillary tube. X-ray diffraction measurement was carried out with a Rigaku AFC7S four-circle diffractometer with graphite-monochromated Mo$K\alpha$ radiation. The cell parameters and an orientation matrix for the data collection were obtained from least-squares refinement using the setting angles of 2θ carefully centered reflections in the range $27.34^o < 2\theta < 29.83^\circ$. The data were collected at 298 ± 1 K using the ω–2θ scan technique to a maximal 2θ value of 70.0°. Omega scans of several intense reflections, made prior to data collection, had an average width at half-height of 0.25°, with a take-off angle of 6.0°. Scans of $(1.00 + 0.30 \tan\theta)^\circ$ were made at the speed of 16.0° min^{-1} (in omega). The weak reflections [$I < 10.0\sigma(I)$] were rescanned (up to five scans) and the counts were accumulated to ensure good counting statistics. Stationary background counts were recorded on each side of the reflection. The ratio of peak counting time to background counting time was 2 : 1. The diameter of the incident beam collimator was 1.0 mm, and the crystal-to-detector distance was 235 mm. The computer-controlled slits were set at 9.0 mm (horizontal) and 13.0 mm (vertical). The crystal structure was solved by a direct method using the program MULTAN88, and expanded by Fourier techniques (9).

Initially all atoms except Na were placed on the positions for an apatite-type structure, i.e., La on the 4*f* and 6*h* sites, Ge on the 6*h* site, and O on the 6*h* and 12*i* sites. Full-matrix least-squares refinements led to an occupancy close to 0.75 for the 4*h* site concerning La (1), but without Na. Therefore, Na was supposed to occupy the same 4*h* site as La (1). A final reliability factor $R = 0.031$ was obtained with all atoms except Na allowed to vibrate anisotropically.

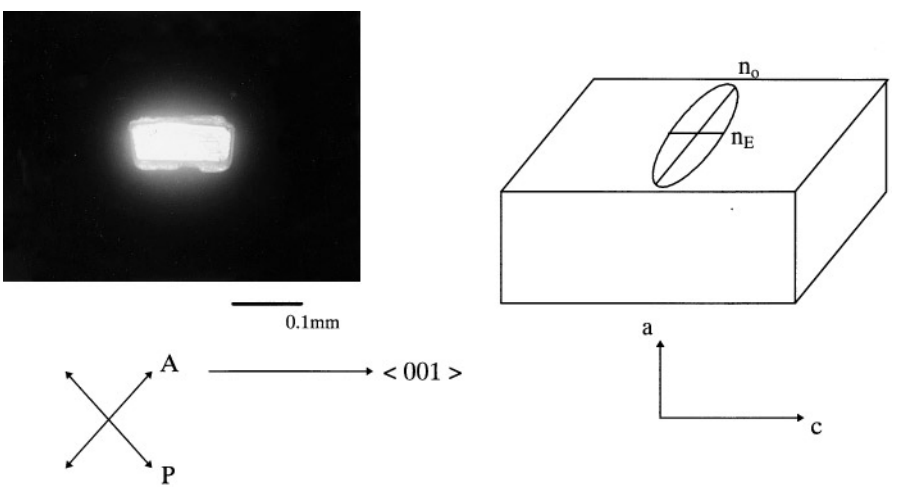

FIG. 2. Optical anisotropy of an oxyapatite $NaLa_9Ge_6O_{26}$ crystal observed by polarized light microscopy with orientation of the optical indicatrix with respect to the crystallographic axis.

3. DISCUSSION

Finer single crystals of apatite $NaLa_9(GeO_4)_6O_2$ with good optical quality (Fig. 2) and without internal stress or inclusions were grown by the flux method, as compared with the melt growth, which resulted in bigger, but irregular, crystals. Single-crystal structure refinements indicated that these two kinds of crystals were identical in structure, but the crystals grown from the high-temperature solution had a better reliability factor ($R = 0.031$) than the crystals obtained from the melt system ($R = 0.037$).

The flux system ($PbO–B_2O_3–Na_2O$) has therefore been shown to be an adequate solvent for the growth of apatite crystals. In fact, that flux provides some advantages: high solubility at relatively low temperatures; low viscosity, $\eta < 10\,mPa\cdot s$ for $PbO–B_2O_3$ mixture (10); low evaporation and virulence; no reactions with Pt crucibles; high solubility of the flux in acid or alkali solutions, affording easier separation of the grown crystals from the solidified flux.

The final atomic parameters and B_{eq} values are listed in Table 2 and the anisotropic displacement parameters in Table 3. The structure of $NaLa_9Ge_6O_{26}$ is found to be very similar to that of $NaY_9Si_6O_{26}$ (2). As stated in the Introduction, the structure of $NaY_9Si_6O_{26}$ included two sets of crystallographically independent positions for Y atoms in the unit cell. One is coordinated by seven O atoms at a mean distance of 0.242 nm, with only one relatively short distance of 0.220 nm. The other is surrounded by nine O atoms at a mean distance of 0.240 nm, with a six of these O atoms at a shorter distance (0.237 nm) and the remaining three O atoms at a longer distance ($\sim$0.278 nm). Therefore, the nine coordinated Y atom sites are very distorted. Like Y atoms in the silicate apatite, the La atoms can also be assigned to two independent sites 4*f* and 6*h* in the unit cell. The atomic distances are listed in Table 4. Figure 3 is the structure model of $NaLa_9Ge_6O_{26}$. The coordination environments of La atoms by O atoms are shown in Fig. 4. The La (1) atom on the 4*f* site is coordinated by nine O atoms. It is linked to the three O(1) atoms at a distance of about 0.2479(3) nm, to the three O(2) atoms at a distance of about 0.2561(4) nm, and to the three O(3) atoms at a distance of about 0.2924(5) nm. Because the distance between La(1) and O(3) is relatively large, the La(1) atom can be also regarded to be in sixfold coordination, the environment of which is fairly distorted from an ideal octahedron. On the other hand, the La(2) atom, which occupies the 6*h* position, is coordinated by seven O atoms, that is O(1), O(2), O(4), and O(3). The distances of the two type bonds between La(2) and O(3) atoms are 0.2618(4) nm $\times$ 2, and 0.2431(4) nm $\times$ 2, respectively. Those between La(2) and O(1), O(2), and O(4) are 0.2732(5), 0.2521(5), and 0.23281(6) nm, respectively. It can be seen that La(2) and O(3) atoms have relatively short bond

TABLE 2
Positional Parameters and B_{eq} Values of $NaLa_9Ge_6O_{26}$

Atom	Site	Occupancy	*x*	*y*	*z*	B_{eq}
La(1)	4*f*	0.750(2)	0.3333	0.6667	0.0003(2)	0.905(6)
Na	4*f*	0.250	0.3333	0.6667	0.0003(2)	0.905(6)
La(2)	6*h*	1.00	0.24157(4)	0.01251(4)	0.25	0.567(5)
Ge	6*h*	1.00	0.37346(7)	0.40143(7)	0.25	0.482(9)
O(1)	6*h*	1.00	0.4867(6)	0.3121(6)	0.25	1.39(8)
O(2)	6*h*	1.00	0.5234(6)	0.3961(5)	0.75	1.13(8)
O(3)	12*i*	1.00	0.2468(4)	0.3407(6)	0.4396(5)	2.33(7)
O(4)	2*a*	1.00	0.0	0.0	0.25	1.07(8)

$B_{eq} = \frac{8}{3}\pi^2(U_{11}(aa^*)^2 + U_{22}(bb^*)^2 + U_{33}(cc^*)^2 + 2U_{12}aa^*bb^*\cos\gamma + 2U_{13}aa^*cc^*\cos\beta + 2U_{23}bb^*cc^*\cos\alpha)$.

TABLE 3
Anisotropic Displacement Parameters[a]

Atom	U_{11}	U_{22}	U_{33}	U_{12}	U_{13}	U_{23}
La(1)	0.0102	0.0102(2)	0.0140(3)	0.0051	0.0	0.0
La(2)	0.0079(1)	0.0080(1)	0.0045(2)	0.00307(8)	0.0	0.0
Ge	0.0068(2)	0.0076(2)	0.0042(3)	0.0039(2)	0.0	0.0
O(1)	0.022(2)	0.026(2)	0.016(3)	0.020(1)	0.0	0.0
O(2)	0.008(2)	0.006(2)	0.024(3)	−0.001(1)	0.0	0.0
O(3)	0.017(1)	0.072(3)	0.007(1)	0.027(1)	0.008(1)	0.020(2)
O(4)	0.0116	0.012(2)	0.018(4)	0.0058	0.0	0.0

[a] General temperature factor expression: $\exp(-2\pi^2(a^{*2}U_{11}h^2 + b^{*2}U_{12}k^2 + c^{*2}U_{33}l^2 + 2a^*b^*U_{12}hk + 2a^*c^*U_{13}hl + 2b^*c^+U_{23}kl))$.

TABLE 4
Bond Lengths and Angles

Atoms	Distance (Å)	Atoms	Angle (°)
Ge–O(1)	1.738(5)	O(1)–Ge–O(2)	115.5(2)
Ge–O(2)	1.733(4)	O(2)–Ge–O(3)	111.4(3)
Ge–O(3) ($\times$2)	1.753(4)	O(3)–Ge–O(1)	110.9(2)
		O(3)–Ge–O(3)	103.6(2)
La(1)–O(1) ($\times$3)	2.479(3)		
La(1)–O(2) ($\times$3)	2.561(4)	O(1)–La(1)–O(1) ($\times$3)	72.1(1)
La(1)–O(4) ($\times$3)	2.924(5)	O(1)–La(1)–O(2) ($\times$3)	94.6(1)
La(2)–O(1)	2.732(5)	O(1)–La(1)–O(2) ($\times$3)	154.9(2)
La(2)–O(2)	2.521(5)	O(1)–La(1)–O(2) ($\times$3)	125.0(1)
La(2)–O(4)	2.3281(6)	O(2)–La(1)–O(2) ($\times$3)	75.3(1)
La(2)–O(3) ($\times$2)	2.618(4)	O(1)–La(2)–O(2)	98.2(2)
La(2)–O(3) ($\times$2)	2.431(4)	O(1)–La(2)–O(3) ($\times$2)	145.0(1)
La(1)–La(1)	3.64	O(1)–La(2)–O(3) ($\times$2)	69.5(1)
La(2)–La(2)	4.032(1)	O(1)–La(2)–O(4)	112.8(1)
		O(2)–La(2)–O(3)	85.82(10)
		O(3)–La(2)–O(3)	63.5(2)
		O(3)–La(2)–O(3)	136.3(2)
		O(3)–La(2)–O(3) ($\times$2)	76.75(8)
		O(3)–La(2)–O(3) ($\times$2)	138.4(1)
		O(4)–La(2)–O(3) ($\times$2)	83.9(1)
		O(4)–La(2)–O(3) ($\times$2)	104.5(1)

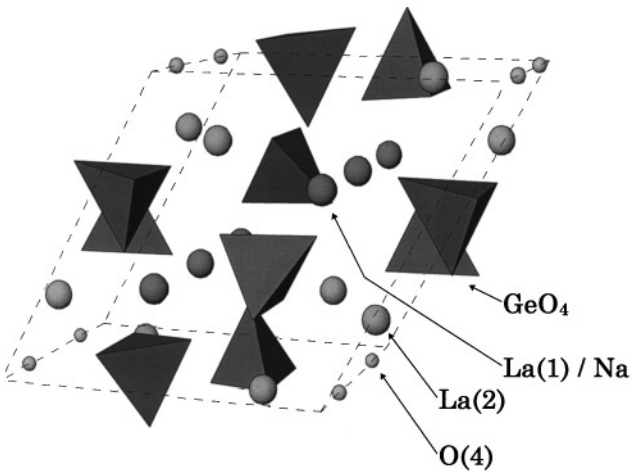

FIG. 3. Apatite-type structure of sodium lanthanum germanate, $NaLa_9Ge_6O_{26}$.

lengths. It is known that bond valences are associated with bond distances. The valence v_{ij} of a bond between two atoms i and j is defined so that the sum of all the valences from a given atom i with valences V_i obeys

$$\sum_j v_{ij} = V_i.$$

The most commonly adopted empirical expression for the variation of the length d_{ij} of a bond with valence is

$$v_{ij} = \exp[(R_{ij} - d_{ij})/b].$$

Here, b is commonly taken to be a "universal" constant equal to 0.37 Å; we use this value of b throughout. And R_{ij} is the bond valence parameter; we use $R_{ij} = 2.172$ for La^{III}–O bonds reported by Brese and O'Keeffe (11). The calculated values of bond valence sums around La(1) and La(2) are listed in Table 5. La(2)–O(4) bonds with small bond valence sums have the highest degree of covalency, whereas La(1)–O(3) bonds with large sums have the highest degree of ionic strength among the La–O bonds.

The site occupancy of La(1) atom was found to be 0.75; therefore, it is supposed that the site occupancy of Na atom is 0.25. This refinement result is consistent with the chemical composition analyzed by EPMA. In general, the apatite structure may contain some Na deficiency. Since the crystals of $NaLa_9Ge_6O_{26}$ were grown from Na-rich solutions, such Na deficiency seems unlikely in these crystals. On the other hand, it was previously suggested that the Na atom on 4*f* sites was favored from electrostatic charge balances (3). The consequence of restricting the O(4) position to $z = 1/4, 3/4$ is that a satisfactory electrostatic charge balance can be achieved by placing La(2) on the 6*h* site. This is in agreement with (3). Moreover, the La(1) site is an ionic site, while La(2) site is a covalent site on the basis of the bond valence sums. So it seems to be that Eu^{3+} ions having small ionic radius are preferred on the La(2) site.

An important structural characteristic of $NaLa_9Ge_6O_{26}$ is that the La–La distances are quite large, i.e., 0.364 nm on nearest-nighbor sites and 0.40324(7) nm on the next-nearest neighbor sites (see Table 4). This fact elicits interest in the potential luminescent properties of this material, especially with respect to the phenomenon of concentration

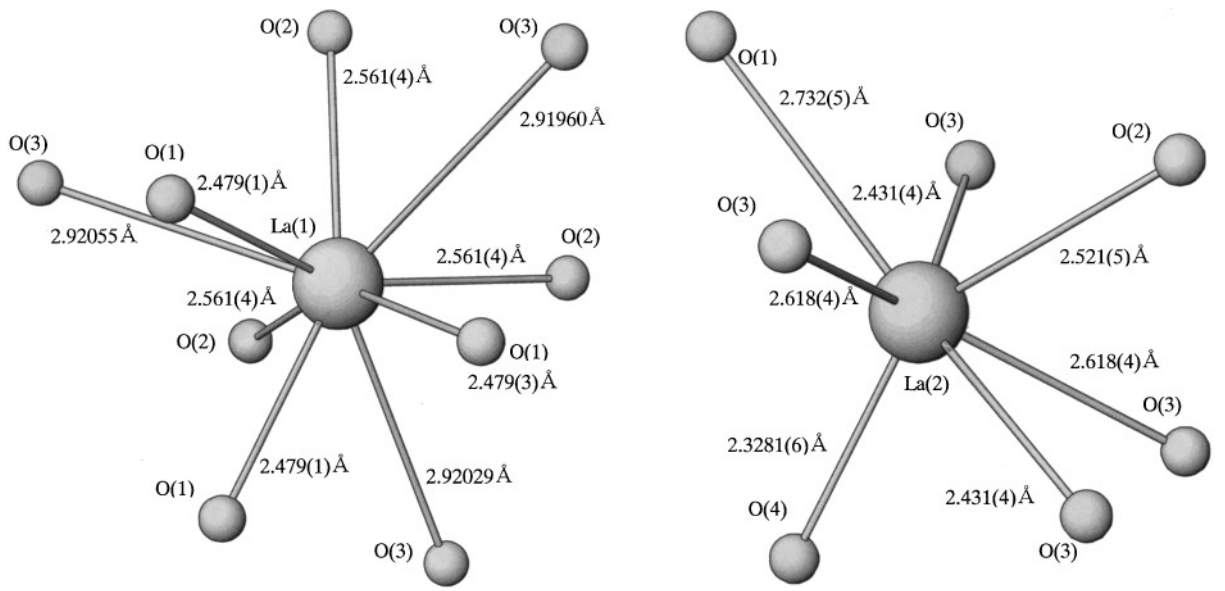

FIG. 4. La atom coordination environments by O atom.

TABLE 5
Calculation of Bond Valence Sums around La1 and La2

Atom	d (Å)	Bond valence v_{ij}
La(1)–O(1) ($\times 3$)	2.479(1)	0.4362×3
La(1)–O(2) ($\times 3$)	2.561(4)	0.3495×3
La(1)–O(3) ($\times 3$)	2.924(5)	0.1310×3
Bond valence sum for La(1)		2.750
La(2)–O(1)	2.732(5)	0.2201
La(2)–O(2)	2.521(5)	0.3894
La(2)–O(3) ($\times 2$)	2.618(4)	0.2996×2
La(2)–O(3) ($\times 2$)	2.431(4)	0.4966×2
La(2)–O(4)	2.3281(6)	0.6558
Bond valence sum for La(2)		2.858

quenching. Concentration quenching usually occurs in phosphors and consists of an actual decrease in luminescence emission intensity with an increase in the amount of activator above an optimal concentration (generally very small). Such effects largely limit further improvement of the phosphor efficiency. The mechanism of concentration quenching is due to energy transfer between the fluorescent ions which have excited states of approximately equal energy and are close together. The critical distance for the energy transfer is considered to be between 0.4 and 0.5 nm from the calculation (12). The La–La distance in the oxyapatite $NaLa_9Ge_6O_{26}$ may exceed the critical distance of concentration quenching. Therefore, by appropriate doping on La sites, we could expect to synthesize new fluorescent materials with stoichiometric compositions. And it is expected that the mechanism of high luminescent efficiency is attributable to the long distance between the fluorescent ions which restricts the excursion of excitation energy by the interactions, the peculiar role as a spacer played by the GeO_4 tetrahedra, and the heavier framework reducing the nonradiative relaxation. Such investigation is in progress.

ACKNOWLEDGMENT

We are very grateful to Mr. Masayoshi Kobayashi (Faculty of Dental Medicine, Niigata University), for help in EPMA analysis.

REFERENCES

1. F. Cervantes, Lee, J. Marr, and F. P. Glasser, *Ceram. Int.* **7**(2), 43 (1981).
2. R. P. Gunawardane, R. A. Howie, and F. P. Glasser, *Acta Crystallogr. Sect. B* **38,** 1564 (1982).
3. G. Blasse, *J. Solid State Chem.* **14,** 181 (1975).
4. M. E. Fleet and Y. M. Pan, *Am. Mineral.* **80,** 329 (1995).
5. C. H. Kim, H. L. Park, and S. Mho, *Solid State Commun.* **101**(2), 109 (1997).
6. D. Elwell and H. J. Scheel, "Crystal Growth from High-Temperature Solutions," p. 102. Academic Press, London, 1975.
7. M. Schieber, *Kristall. Tech.* **2,** 55 (1967).
8. R. E. Newnham, "Structure–Property Relations," p. 118. Springer-Verlag, Berlin, 1975.
9. T. Debaerdemaeker, G. Germain, P. Main, L. S. Refaat, C. Tate, and M. M. Woolfson, "Computer Programs for the Automatic Solution of Crystal Structure from X-ray Diffraction Data," University of York, 1988.
10. K. Watanabe, *Bull. Ceram. Soc. Japan* **31** (6), 495 (1996).
11. N. E. Brese and M. O'Keeffe, *Acta Crystallogr. Sect. B* **47,** 192 (1991).
12. A. J. De Vries, H. S. Kiliaan, and G. Blasse, *J. Solid State Chem.* **65,** 190 (1986).